All-Optical THz OFDM Communications using Photonic Crystal Fibers

Sai Venkatesh Balasubramanian

Sree Sai Vidhya Mandhir, Mallasandra, Bengaluru-560109, Karnataka, India.
saivenkateshbalasubramanian@gmail.com

Abstract

An all-optical Orthogonal Frequency Division Multiplexing communication system at 2 THz is modeled using photonic crystal fiber of length 1km, and the performance of four carrier waveforms - hyperbolic secant, square of hyperbolic secant, square and sinusoidal is evaluated using standard metrics such as eye diagram and bit error rate. From the above mentioned valuations, one can deduce the minimal distortion in hyperbolic secant based carriers, hence leading to unconventional carrier waveforms, which forms the novelty of the present work.

Keywords: Nonlinear optics, Optical fiber communication, OFDM, Optical pulses, Amplitude Shift Keying

1. Introduction

Recent trends show an ever-increasing demand for instant and reliable communication, with faster data rates. The consequence is that photonic components are increasingly finding applications in high frequency communications systems. As optical fibers have advanced in leaps and bounds in recent times, a particular group of fibers, the photonic crystal fibers (PCF) emerge as the forerunners in high frequency robust communication systems [1]. Because of its ability to confine light, or with confinement characteristics not possible in conventional optical fiber, PCF is now finding applications in fiber-optic communications [2, 3], fiber lasers [4], nonlinear devices [5], highly sensitive sensors [6], and other areas. This is perhaps the single most successful fiber design to date based on structuring the fiber design using air holes and has important applications regarding high numerical aperture and light collection especially when implemented in laser form, but with great promise in areas as diverse as biophotonics [7]. [18] also discusses Liquid-Core PCF, which provides better robustness against perturbations.

One of the fast-developing regions of the electromagnetic spectrum is the Terahertz range, also called as millimeter waves. Terahertz (THz) waves offer tens and hundreds of gigahertz bandwidths [8, 9], and it is shown that this frequency band unlike Microwaves, is only a minor health threat [8, 9]. The main issue for THz wave propagation is atmospheric attenuation, which is dominated by water vapor absorption in the THz frequency band. From experiments on the propagation of THz waves in air, it is observed that there are a number of THz transmission windows [8, 9].

When modulation of any form - voice, data, etc. is applied to a carrier, then sidebands spread out either side. It is necessary for a receiver to be able to receive the whole signal to be able to successfully demodulate the data. As a result when signals are transmitted close to one another they must be spaced so that the receiver can separate them using a filter and there must be a guard band between them. This is not the case with Orthogonal Frequency Division Multiplexing (OFDM) which is a popular modulation format in present radio communications [10]. An OFDM signal consists of a number of closely spaced modulated carriers. Although the sidebands from each carrier overlap, they can still be received without the interference that might be expected because they are orthogonal to each another. This is achieved by having the carrier spacing equal to the reciprocal of the symbol period [11].

The distribution of the data across a large number of carriers in the OFDM signal has some further advantages. Nulls caused by multi-path effects or interference on a given frequency only affect a small number of the carriers, the remaining ones being received correctly. By using error control coding techniques, that add further data to the transmitted signal, it enables many or all of the corrupted data to be reconstructed within the receiver. This can be done because the error correction code is transmitted in a different part of the signal. Reed-Solomon Error Control Coding of (n,k) of (255,233) is used along with random interleaving to boost the efficiency of the system [12, 13].

The present work models an all-optical communication system based on OFDM, using photonic crystal fibers as the channel, and evaluates the robustness of four carrier waveforms the hyperbolic secant, square of hyperbolic secant, Sinusoidal, and Square waves. The modulation technique used here is amplitude shift keying (ASK) [13]. The propagation of hyperbolic secant pulses with digital modulation techniques at Terahertz frequencies forms the novelty of the present work.

2. Methodology

In the present work, OFDM with cyclic prefix is used. A block diagram illustrating the proposed communication system is shown in Fig.(1), and the components, namely, transmitter, channel and receiver, are explained as follows.

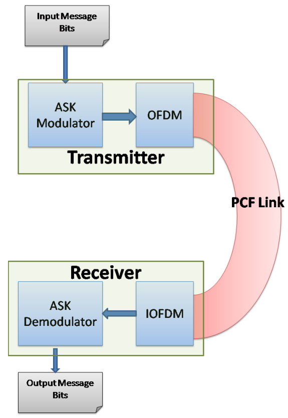

Figure 1: Block Diagram of all-optical OFDM system

2.1. Transmitter

The transmitter component consists of a message generator, modulator and OFDM Multiplexer. The message generator is modeled by a sequence of randomly generated bits, and Reed-Solomon error control coding is then applied to this bit stream, where the codeword size 'n' and message size 'k' are chosen as 255 and 233 respectively.

The modulation schemes used in the present work is Amplitude Shift Keying(ASK), and hence the output of the message generator is fed to the ASK modulator. In digital modulation, an analog carrier signal is modulated by a discrete signal. In ASK, the amplitude of an analog carrier signal varies in accordance with the bit stream (modulating signal), keeping frequency and phase constant[13]. One can think of data signal as an ON or OFF switch. In the modulated signal, logic '0' is represented by the absence of a carrier, and logic '1' by the presence of the carrier, thus giving OFF/ON keying operation and hence the name (On-Off Keying) OOK is given.

In the present work, the ASK modulator is represented as a generic mathematical model where, a choice of carrier is made at runtime, and depending on the choice made, the ASK modulator outputs one cycle of the carrier for every logical '1' and zero amplitude for every logical '0' [13, 14, 15].

The output of the ASK modulator is then Multiplexed using an OFDM Multiplexer block. This is mathematically represented by a serial-to-parallel converter, an Inverse Fourier Transform block (IFFT) and a cyclic prefix block in series. The output of this block is an OFDM waveform, characterised by a spread spectrum, where the ultra wide band helps in counteracting signal fading effects [14, 15].

2.2. Channel

The Channel of the proposed communication system is a photonic crystal fiber link operating at the terahertz regime. The nonlinear pulse propagation equation in the time domain in a PCF is given by the generalized nonlinear Schrödinger equation, which is shown in Eq.(1) [16, 17].

$$\begin{aligned}\frac{\partial A}{\partial z} &+ \frac{\alpha}{2}A + \frac{i\beta_2}{2}\frac{\partial^2 A}{\partial T^2} - \frac{\beta_3}{6}\frac{\partial^3 A}{\partial T^3} - \frac{i\beta_4}{24}\frac{\partial^4 A}{\partial T^4} \\ &= i\gamma\left(1 + \frac{i}{\omega_0}\frac{\partial}{\partial T}\right)\varpi(z,T), \\ R(t) &= (1-f_R)\delta(t) + f_R h_R(t)\text{and} \\ h_R(t) &= \frac{\tau_1^2+\tau_2^2}{\tau_1\tau_2^2}\exp(-t/\tau_2)\sin(t/\tau_1), \qquad (1)\end{aligned}$$

where $T = t - \beta_1 z$, and

$$\varpi(z,T) = \left(A(z,T)\int_{-\infty}^{\infty} R(T')|A(z,T-T')|^2 dT'\right). \qquad (2)$$

Here β_2, β_3 and β_4 correspond to the group velocity dispersion (GVD) coefficient, third order dispersion coefficient, and fourth order dispersion coefficient respectively. α is the confinement loss and γ is the nonlinear parameter responsible for self phase modulation. $R(t)$ is the Raman response function, and the fractional contribution of the delayed Raman response for silica core PCF is $f_R = 0.18$. Also, for standard silica PCF, $\tau_1 = 12.2$fs and $\tau_2 = 32$ fs[16].

Since four types of pulses, namely soliton, similariton, square and sinusoid are considered, the values for β and γ are determined for terahertz propagation of solitons from [18] with a FWHM pulse width of 56.5fs and a central wavelength of 850nm [18]. A Silica Core PCF is considered, where the small pitch Λ is taken as 1μm and the diameter-pitch ratio, d/Λ is given as 0.6. Such a photonic crystal fiber exhibits a Zero Dispersion wavelength of 742nm, and the Group Velocity Dispersion of 110.26 ps/nm at the operating wavelength of 850nm. The values for Dispersion constants β_2, β_3, and β_4 are given as -0.0104 ps^2/m, $3.78 \times 10^{-5} ps^3$/m, and $1.02 \times 10^{-6} ps^4$/m respectively [18]. The nonlinear factor γ is given as 0.1518 $W^{-1}m^{-1}$ [18], and the confinement loss α is given as 0.019 dB/m [18]. The pulse power is set to 68W [18].

Incorporating the above-mentioned values, the generalized nonlinear Schrödinger equation is numerically solved using the Predictor Corrector Symmetrized Split Step Fourier method (PC-S-SSFM) [19]. The SSFM method relies on computing the solution in small steps, and treating the linear and the nonlinear steps separately. It is necessary to Fourier transform back and forth because the linear step is made in the frequency domain while the nonlinear step is made in the time domain.

The fiber link length is taken as 1km, and the number of steps is chosen as 3000. The sampling time is set to 1fs.

2.3. Receiver

The receiver component consists of three parts, an OFDM demultiplexer (IOFDM) [14, 15], an ASK Demodulator, and the output message decoder. The OFDM demultiplexer performs the inverse operation of the multiplexer and combines the various subcarriers into a single waveform. For this purpose, it is modeled as a series combination of a Cyclic prefix remover, a Fast Fourier Transform block (FFT), and a parallel-to-serial converter. The output of this block is fed to ASK demodulator which is mathematically modeled to give a logic '1' when carrier presence is detected and logical '0' when no carrier is detected. This generates a bit stream on which the error control decoding and detection is applied. The result is a bit stream that is the output of the communication system.

3. Results and Discussions

The All-Optical OFDM system is modeled in MATLAB for different carrier waveforms, at a frequency of 2THz, for a PCF length of 1km. For sech and sech squared pulses, the pulse width is 56.5fs. The modeling of the signal generation is done in three stages. In the first stage, the input message signal is modeled as a random bit sequence. The second stage consists of Amplitude Shift Keying modulation, where each bit determines the amplitude of one cycle of the carrier waveform. The carrier waveform is designed at a repetition rate of 2THz, and since each bit modulates one cycle of the carrier, the transmitted bit rate is 2Tbps. The output of this stage is a modified train of the carrier (sech, square of sech,sine or square),with the carrier cycles existing when the bit is a '1' and zero amplitude when the bit is a '0'. The third stage consists of multiplexing the modulated waveform using the OFDM technique, which splits the waveforms into a series of subcarriers. This results in broadening of the waveform spectrum which helps to counteract fading effects and increase the channel capacity [11]. The OFDM spectrum is shown in Fig.(2). Following this, the photonic crystal

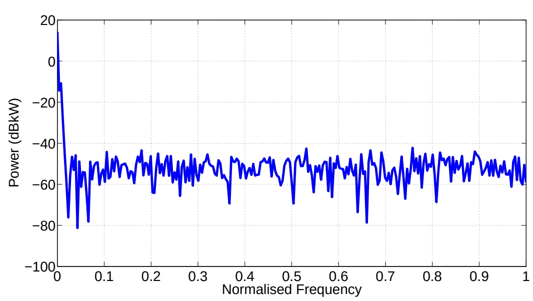

Figure 2: OFDM spectrum

fiber is modeled using the Predictor-Corrector Split Step Fourier Method for a length of 1km. For the case of solitary waves (sech pulses), the fiber properties of group velocity dispersion and nonlinearity are taken from [18]. The stages of modulation and multiplexing are reversed in the receiver end to get back the message. The transmitted bit streams for message lengths of 2^7 bits and 2^{28} bits are plotted vis-a-vis the corresponding received bit streams and this is shown in Figs.(3)-(4)respectively.

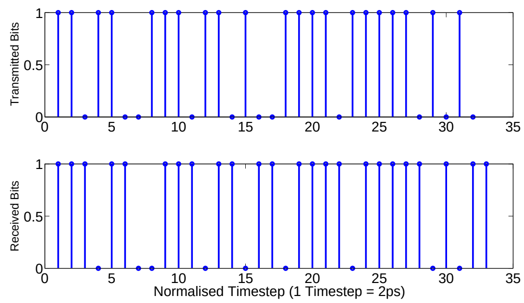

Figure 3: Transmitted and received bit streams of length 2^7

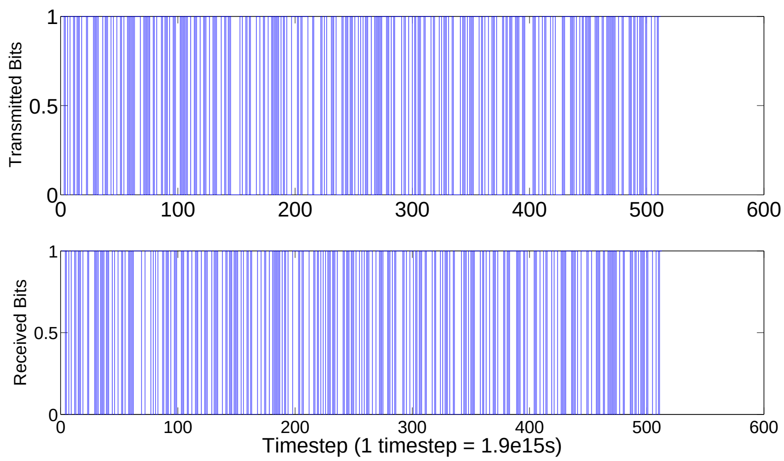

Figure 4: Transmitted and received bit streams of length 2^{28}

The performance of the system is assessed by using two important metrics, the eye-diagram and the Bit Error Rate (the fraction of erroneous bits). The Eye diagram is a superimposition of wave cycles for all the bits [16].

3.1. Analysis of sech carrier

A sample of the modulated signal for the first four bits is illustrated in Fig.(5). The eye diagram of the received signal for a message length of 2^{28} bits, are shown in Fig.(6). As can be seen from the eye diagrams, a large eye height corresponding to minimal distortion is obtained.

3.2. Analysis of square of sech carrier

The first four bits of the modulated signal is illustrated in Fig.(7). The eye diagram of the received signal for a message length of 2^{28} bits, are shown in Fig.(8). Similar to the case of sech waves, very minimal distortion is observed here as well.

3.3. Analysis of square carrier

The modulated signal for the first four bits is illustrated in Fig.(9). The eye diagram of the received signal for a message length of 2^{28} bits, are shown in Fig.(10). The eye height of the square signal is very small indicating a high amount of distortion. This distortion can be attributed to the attenuation of the higher frequency components of a square carrier during propagation in a fiber.

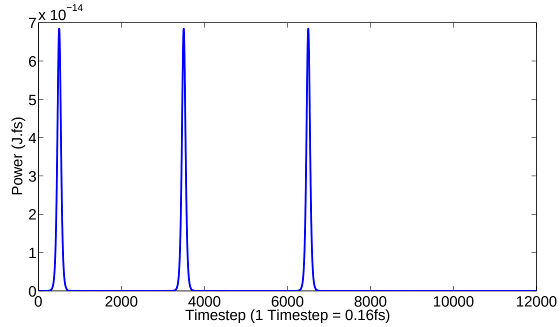

Figure 5: ASK Modulated waveform of sech

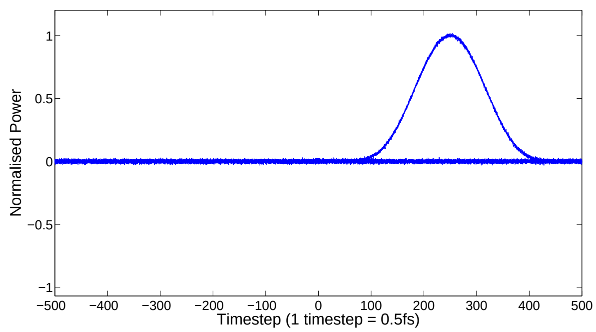

Figure 6: Eye diagram for hyperbolic secant carrier

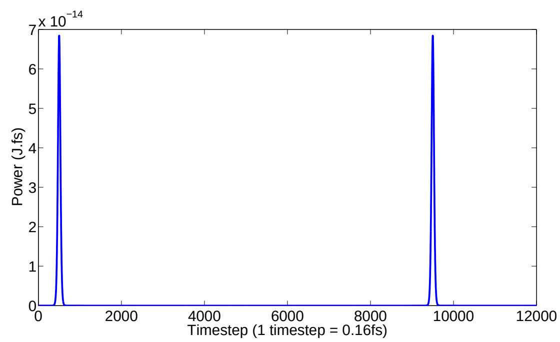

Figure 7: ASK Modulated waveform of square of sech

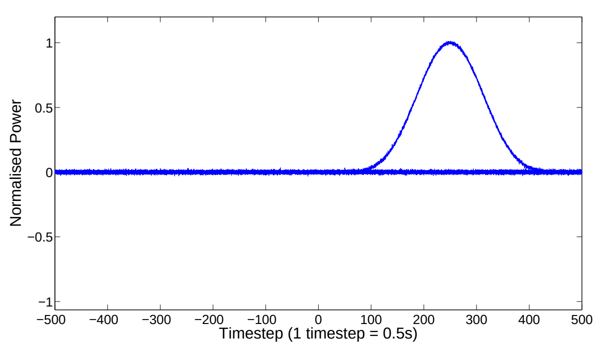

Figure 8: Eye diagram for square of hyperbolic secant carrier

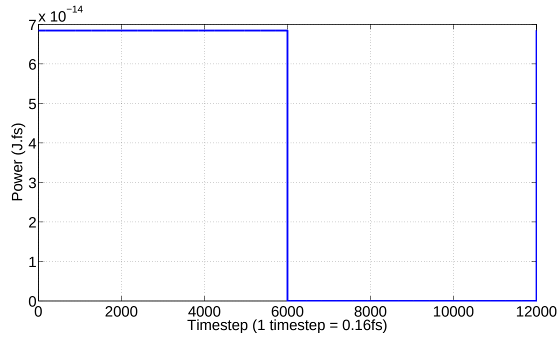

Figure 9: ASK Modulated waveform of square

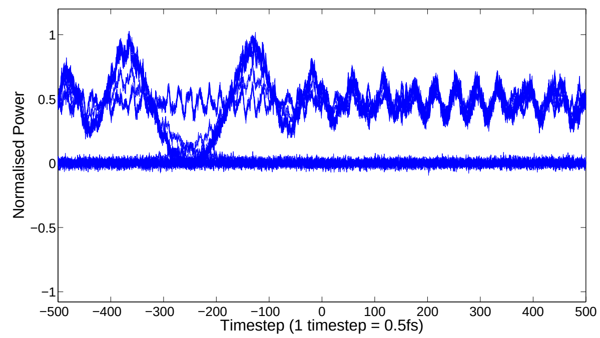

Figure 10: Eye diagram for square carrier

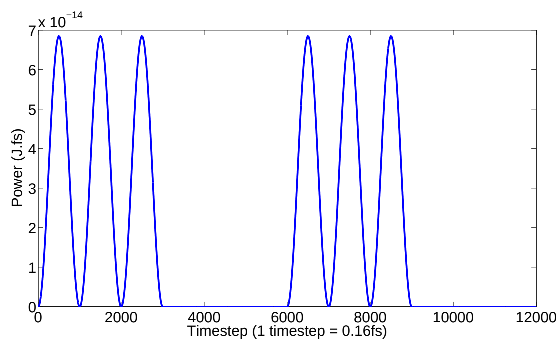

Figure 11: ASK Modulated waveform of sinusoid

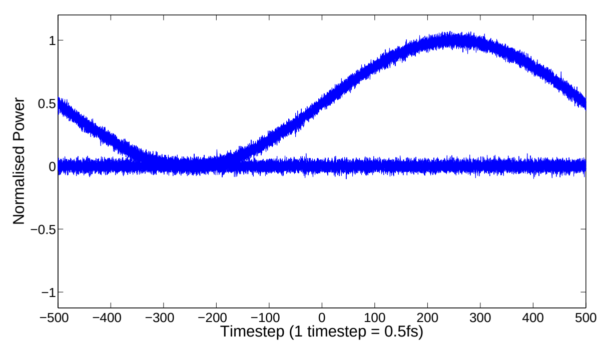

Figure 12: Eye diagram for sinusoidal carrier

3.4. Analysis of sine carrier

The modulated signal for the first four bits is illustrated in Fig.(11). The eye diagram of the received signal for a message length of 2^{28} bits, are shown in Fig.(12). Similar to the case of square carriers, sine carriers also experience considerable amount of distortion.

It is clearly seen that the relative eye-height of the square and sinusoidal are considerably reduced whereas the hyperbolic secant based pulses are more robust carrier candidates. The bit error rate for the sech, square of sech, square and sine waveforms are obtained as 0.03, 0.07, 0.47 and 0.18 respectively, again reinforcing the fact that hyperbolic secant waveforms considerably outperform the square and sine counterparts.

The variations of bit error rate for all four carrier waveform choices are recorded for different bit lengths, ranging from 2^7 bits to 2^{28} bits and plotted in Fig. (13). From these plots, one can observe that the variation of error rate is not significant with respect to message length, thus emphasising the robustness of the valuation schemes. Also, one can observe the consistent low distortion in the performance of secant based carrier waveforms, characterised by the low bit error rate.

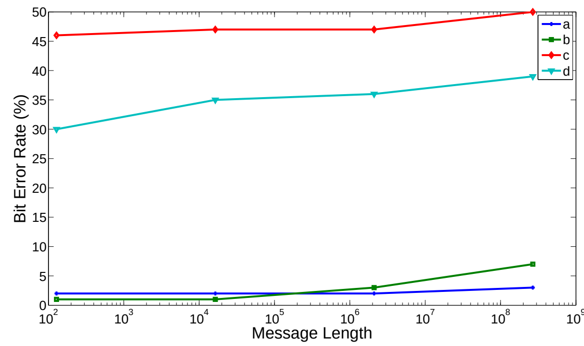

Figure 13: Variation of Bit Error Rate, as a function of Message length for (a) sech, (b) square of sech, (c) square and (d) sinusoidal carriers.

Similarly, the variations of bit error rate for all four carrier waveform choices are recorded for different input powers ranging from microwatts to kilowatt values in Fig. (14). From this graph, one can observe the low distortion of secant based carriers throughout different power levels, this characterised by the low bit error rate values. At high power levels (above 1kW), due to the random nature of distortion caused in all four carriers, the variations of bit error rate show some degree of erratic variations.

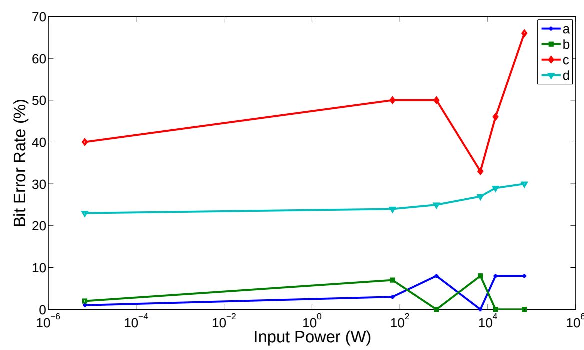

Figure 14: Variation of Bit Error Rate, as a function of Input Power for (a) sech, (b) square of sech, (c) square and (d) sinusoidal carriers.

From the above analysis, one can clearly infer the better performance of hyperbolic secant based carriers in both bit error rates and eye heights, for a wide range of variations in message length and signal power.

4. Conclusion

A model of an all-optical OFDM system based on photonic crystal fiber has been developed that describes fairly accurately, the various channel effects. It is evident from the results that hyperbolic secant pulses are relatively robust carriers for THz communications compared to squares/sinusoidal carriers and this may enable a distortion free communication system, even in the worst possible SNR levels. The modulation scheme chosen here is ASK in order to avoid phase complexities in split-step Fourier method calculations. This can be extended in future to include other phase-based modulation schemes such as bipolar phase (BPSK) and Quadrature phase (QPSK).

The PCF based all-optical OFDM system forms the cornerstone of futuristic Radio-Over-Fiber based Communication systems, where conventional wireless and mobile communication systems are replaced by fiber-links between the central stations and the regional base stations. Such systems can hence be designed with the help of the PCF link modeled in the present work, with modulation based on non-conventional hyperbolic secant carriers operating in the Terahertz regime, and this forms the novelty of the present work.

References

[1] J.C.Knight. Photonic crystal fiber. Nature. 2003;424:847-851.
[2] H.Masaaki. Future of Transmission Fiber. IEEE Photonics Journal. 2011;3:316-319.
[3] K.Kurokawa, K.Nakajima, K.Tsujikawa, Y.Yamamoto and K.Tajima. Ultra-Wideband Transmission Over Low Loss PCF. IEEE.J.Lightwave.Tech. 2009;27:1653-1662.
[4] J.A.Sanchez Martin, J.M.A.Abenia, M.A.Rebolledo, M.V.Andres and A.Diez. Amplifiers and Lasers Based on Erbium-Doped Photonic Crystal Fiber: Simulation and Experiments. IEEE.J.Quantum Electronics. 2012;48:338-344.
[5] T.Uthayakumar, R.V.J.Raja, and K.Porsezian. All-Optical Steering of Light Through Nonlinear Twin-Core Photonic Crystal Fiber Coupler at 850 nm. IEEE.J.Lightwave Tech. 2012;30:2110-2116.
[6] W.J.Bock, J.Chen, T.Eftimov, W.Urbanczyk. A photonic crystal fiber sensor for pressure measurements. IEEE Transactions on Instrumentation and Measurement. 2006;55:1119-1123.
[7] D.J.J.Hu, J.L.Jim, M.K.Park, L.T.H.Kao, Y.Wang, H.Wei and W.Tong. Photonic Crystal Fiber based interferometric Biosensor for Streptavidin and Biotin Detection. IEEE.Journal of Selected Topics in Quantum Electronics. 2012;18:1293-1297.
[8] X.C.Zhang and J.Xu. Introduction to THz Wave Photonics. USA: Springer; 2010.
[9] A.Rostami, H.Rasooli and H.Baghban. Terahertz Technology Fundamentals and Applications. Germany: Springer; 2011.
[10] H.Rohling. OFDM: Concepts for future Communication systems. Germany: Springer; 2011.
[11] W.Sheih and I.Djordjevic. Orthogonal Frequency Divison Multiplexing for Optical Communications. Burlington: Elsevier; 2010.
[12] L.Shu, S.Lin and D.J.Costello. Error Control Coding. UK: Pearson; 2005.
[13] B.Sklar. Digital Communications: Fundamentals and Applications. California: Pearson; 2010.
[14] S.D.Dissanayake and J.Armstrong. Comparison of ACO-OFDM, DCO-OFDM and ADO-OFDM in IM/DD Systems. IEEE.J.Lightwave Tech. 2013;31:1063-1072.
[15] J.Armstrong. OFDM for Optical Communications. IEEE.J.Lightwave Tech. 2009;27:189-204.
[16] J.Dudley and R.Taylor. Supercontinuum generation in optical fibers. UK: Cambridge University Press; 2010.
[17] R.Deiterding. A Reliable Split-Step Fourier Method for the Propagation Equation of Ultra-Fast Pulses in Single-Mode Optical Fibers. IEEE.J.Lightwave Tech. 2013;31:2008-2017.
[18] R.V.J.Raja, K.Porsezian, S.K.Varshney and S.Sivabalan. Modeling photonic crystal fiber for efficient soliton pulse propagation at 850nm. Optics Communications. 2010;283:5000-5006.
[19] X.Liu and B.Lee. A Fast method for nonlinear Schrödinger Equation. IEEE Photon. Technol. Lett. 2003;15:1549-1551.
[20] Y.S.Kivshar and G.Agarwal. Optical Solitons: From Fibers to Photonic Crystals. USA: Academic Press; 2013.